Scientific article
UDC 547.82
DOI: 10.52957/2782-1900-2024-5-2-101-108

REGIOSELECTIVITY OF 9-CHLOROPYRIDO[1,2-*a*]BENZIMIDAZOLE HALOGENATION REACTION

R. S. Begunov, L. I. Savina

Roman S. Begunov, Candidate of Chemical Sciences, Associate Professor; **Luisa I. Savina**, Student
P.G. Demidov Yaroslavl State University, Yaroslavl, Russia
begunov@bio.ac.ru, luizasavina2000@mail.ru

Keywords:
*9-chloropyrido[1,2-a]benzimidazole, N-halogensuccinimide, S_EAr reaction, regioselectivity, quantum chemical modelling, DFT method B3LYP/6-31G**, PC GAMESS/Firefly and ORCA 5.0.4 software applications*

Abstract: *This paper describes the S_EAr regioselectivity of the 9-chloropyrido[1,2-a]benzimidazole reaction by experimental and quantum chemistry methods. We conducted the halogenation process in sulfuric acid using N-bromosuccin- or N-chlorosuccinimide. Two isomeric products 8-Hal-9-chloropyrido[1,2-a]benzimidazole and 6-Hal-9-chloropyrido[1,2-a]benzimidazole occurred. Predominantly, the introduction of the electrophilic particle occurred at the 8th position of the heterocycle. Using quantum chemistry methods, we found the orbital control of the electrophilic halogenation reaction and determined the orientation of the electrophile particle introduction by the distribution of the boundary electron density in the substrate. This corresponded well with the experimental data.*

For citation:
Begunov, R.S. & Savina, L.I. (2024) Regioselectivity of 9-chloropyrido[1,2-*a*]benzimidazole halogenation reaction, *From Chemistry Towards Technology Step-By-Step,* 5(2), pp. 101-108 [online]. Available at: https://chemintech.ru/ru/nauka/issue/5176/view

Introduction

Pyrido[1,2-*a*]benzimidazoles are the prospective compounds for the new drugs production. This heterocyclic nucleus is a part of substances exhibiting various types of biological activity: antimalarial [1], antitumour [2], oncoprotective [3], and antiviral ones [4]. Therefore, pyrido[1,2-*a*]benzimidazole derivatives with antimicrobial activity are of particular interest [5]. Thus, a number of effective antibiotics based on rifaximin containing this heterocycle in its structure have been developed [6].

According to numerous experimental data, introduction of halogen atoms into azaheterocyclic systems show enhancing of their biological activity [7-9]. For example, the paper [7] shows increasing in the number of halogen atoms in an azagetheroaromatic system enhanced the antimicrobial effect and also decreased the value of the minimum inhibitory concentration. Also, [9] reported a two or more fold decrease in the required concentration for inhibition of fungal cultures in the presence of halogens in the compound structure.

The simplest way to synthesis halogen derivatives of pyrido[1,2-*a*]benzimidazoles represents the introduction of halogen atoms under the electrophilic aromatic substitution reaction conditions. However, due to the small amount of data on the reactivity of pyrido[1,2-*a*]benzimidazoles in the S_EAr reaction, this method has not yet been widely used in organic synthesis.

We have previously studied the regioselectivity of the nitration and halogenation reaction of 7-R-pyrido[1,2-*a*]benzimidazoles (R = Cl or electron acceptor groups) [10]. Introduction of the electrophilic particle occurred in the 8th position of the heterocycle. The second reaction centre for electrophilic attack at R = Cl was the 6th position. 9-Substituted derivative was not obtained during the S_EAr reaction.

We used 9-chloropyrido[1,2-*a*]benzimidazole (**1**) as a substrate for further studying the regularities of this chemical process and obtaining of a polyhalogen derivative of pyrido[1,2-*a*]benzimidazole. It contains halogen atoms including those at the 9th position.

Main body

We conducted the synthesis of 9-chloropyrido[1,2-*a*]benzimidazole (**1**) according to the previously developed methodology [11, 12] under the conditions of reductive intramolecular heterocyclisation reaction.

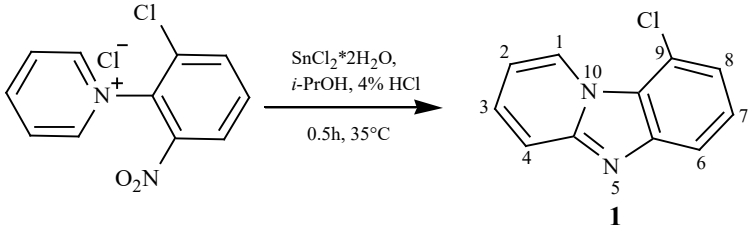

1

The structure of **1** was proved by ^1H, ^{13}C NMR spectroscopy and high-resolution mass spectrometry. We determined the assignment of proton and carbon atom signals from 2D ^1H-^1H NOESY, 2D ^1H-^{13}C HSQC (Fig. 1, left), and 2D ^1H-^{15}N HMBC spectra (Fig. 1, right).

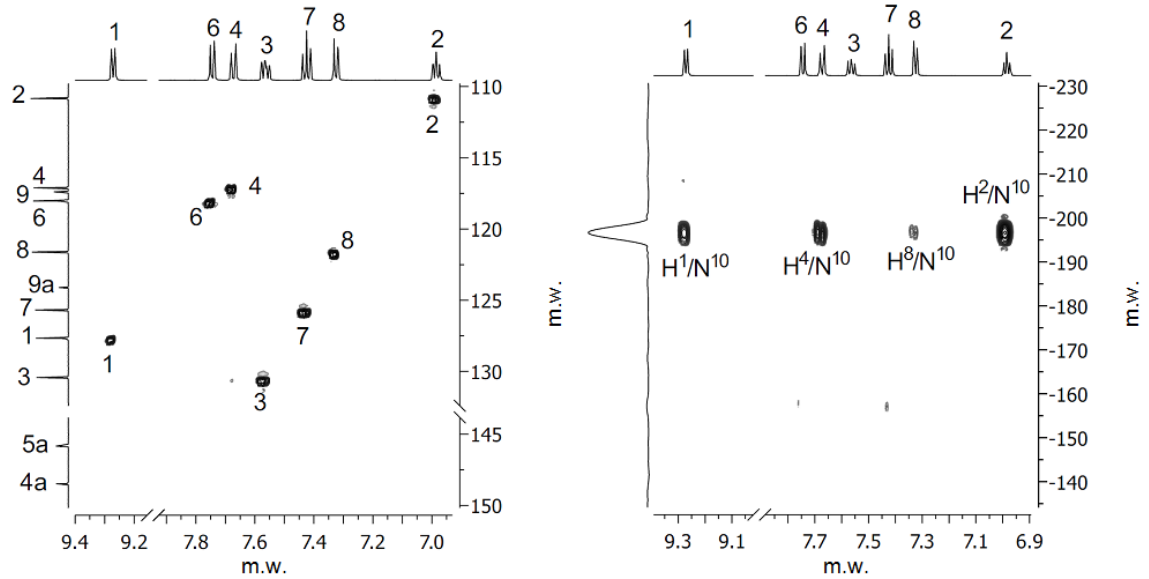

Fig. 1. Fragments of ^1H-^{13}C HSQC (left) and ^1H-^{15}N HMBC (right) spectra of 9-chloropyrido[1,2-*a*]benzimidazole (1)

The use of heteronuclear single-quantum (HSQC) and multijunction (HMBC) correlation spectroscopy allowed the identification of the H^8 signal associated with C^8, which is one of the possible reaction centres for electrophilic attack.

We added bromine and chlorine atoms to the 9-chloropyrido[1,2-*a*]benzimidazole molecule (**1**) in concentrated H_2SO_4 using N-bromosuccinimide (**2a**) or N-chlorosuccinimide (**2b**).

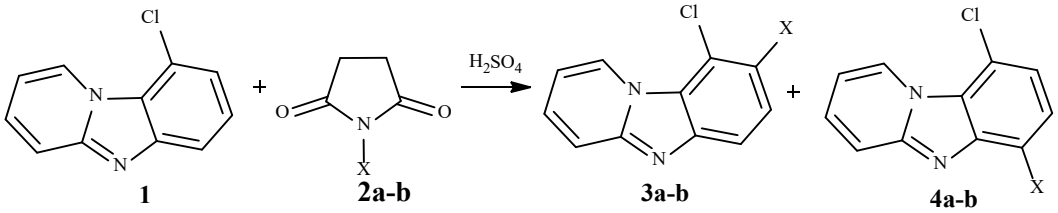

where X = a) Br; b) Cl

We put solutions of halogenating agent **2a** and substrate **1**, taken in equimolar amounts, simultaneously into the reactor at 30 °C. We conducted the reaction for 20 h. Analysis of the obtained reaction mass by ^{1}H NMR spectroscopy showed the presence of two products 8-bromo-9-chloropyrido[1,2-*a*]benzimidazole (**3a**) and 6-bromo-9-chloropyrido[1,2-*a*]benzimidazole (**4a**) in the ratio **3a** : **4a** = 1 : 0.47. Approximately 40 per cent of the starting substance remained unreacted. We obtained similar results using **2b** and observed the formation of two isomers of 8,9-dichloropyrido[1,2-*a*]benzimidazole (**3b**) and 6,9-dichloropyrido[1,2-*a*]benzimidazole (**4b**) at the ratio **3b** : **4b** = 1 : 0.37. The chlorination reaction was slower. Conversion **1** was only 22 %.

The amount of unreacted starting substance **1** in the bromination and chlorination reactions decreased with increasing the time to 30 h and the reaction temperature S_EAr to 50 °C but remained significant. The conversion of **1** was more affected by increasing the amount of halogenating agent in the reaction mass. Thus, 100% conversion of compound **1** was observed at a ratio of **1** : **2a** = 1 : 1.4 and **1** : **2b** = 1 : 3.0.

We added a S_EAr solution of the halogenating agent in H_2SO_4 gradually for 10 h at 45 °C to increase the regioselectivity of the reaction. Then we stirred the reaction mixture at this temperature for another 10 h. The 8,9-dihalogenpyrido[1,2-*a*]benzimidazoles (**3a,b**) were obtained with 89 and 87% yield, respectively, after recrystallisation in chloroform.

The structure of dihalogen derivatives **3** was proved by ^{1}H, ^{13}C NMR spectroscopy and high-resolution mass spectrometry. We determined the assignment of proton and carbon atom signals from 2D ^{1}H-^{1}H NOESY, 2D ^{1}H-^{13}C HSQC, and 2D ^{1}H-^{15}N HMBC spectra. Fig. 2 shows fragments of the ^{1}H-^{13}C HSQC (left) and ^{1}H-^{15}N HMBC (right) spectra of 8,9-dichloropyrido[1,2-*a*]benzimidazole (**3b**).

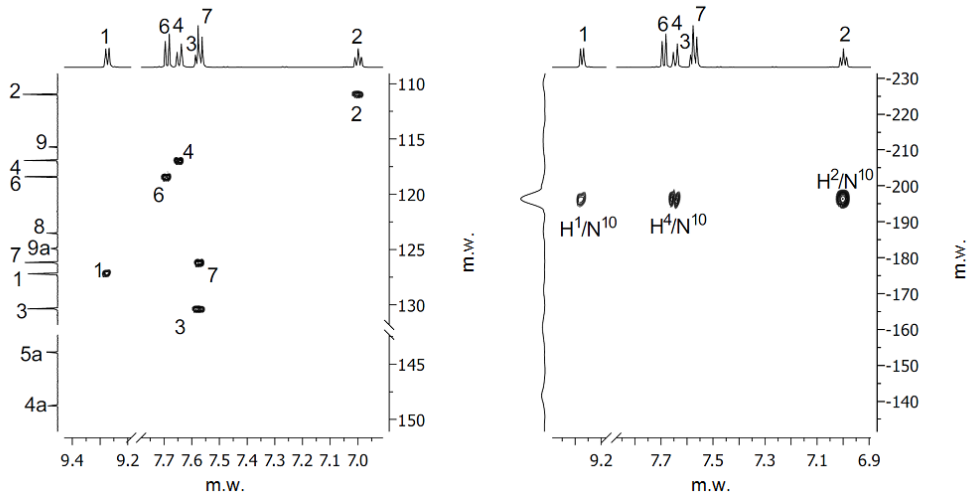

Fig. 2. Fragments of ^{1}H-^{13}C HSQC (left) and ^{1}H-^{15}N HMBC (right) spectra of 8,9-dichloropyrido[1,2-*a*]benzimidazole (**1**)

There were no H^8/C^8 and H^8/N^{10} interaction cross-peaks in the ^{1}H-^{13}C HSQC and ^{1}H-^{15}N HMBC spectra of this compound, which were observed for substrate **1**. This indicated the substitution of a hydrogen atom for a halogen in the 8th position of the heterocycle.

Thus, the introduction of the electrophilic particle occurred predominantly in the *ortho*-position rather than the *para*-position relative to the substituent, contrary to the *-I*-effect of the chlorine atom.

We calculated the charge and orbital characteristics of 9-halogenpyrido[1,2-*a*]benzimidazole (**1**) and its imide nitrogen protonated heterocyclic derivative (**1'**) in order to explain the orientation of the S_EAr reaction using the B3LYP/6-31G** method. We performed the calculations within the density functional theory with hybrid exchange-correlation functions [13-15] (DFT B3LYP/6-31G** method) for open electron shells [15] using the PC GAMESS/Firefly software package [16] and the ORCA 5.0.4 programme [17]. We performed geometry optimisation both in the gas phase and using a discrete SMD solvation model. We used water as a solvating shell. Table 1 and Table 2 present the results of calculations.

Table 1. Charges and boundary electron densities on C atoms in the HOMO of 9-chloropyrido[1,2-*a*]benzimidazole (**1**)

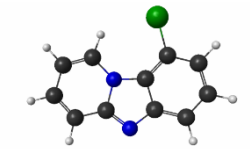

Number of atom	Charges on C	Boundary electron densities on C in HOMO	Charges on C (including solvation)	Boundary electron densities on C in HOMO (including solvation)
C^1	0.14079	0.10956	0.05368	0.09143
C^2	-0.15330	0.09383	-0.20670	0.07990
C^3	-0.06353	0.07206	-0.11925	0.05012
C^4	-0.12548	0.12162	-0.20686	0.10033
C^6	-0.11755	**0.15708**	-0.21034	**0.12035**
C^7	-0.08905	0.00784	-0.15481	0.00553
C^8	-0.10077	**0.15710**	-0.17739	**0.13071**

Table 2. Charges and boundary electron densities on C atoms in the HOMO of 9-chloropyrido[1,2-*a*]benzimidazole (**1'**)

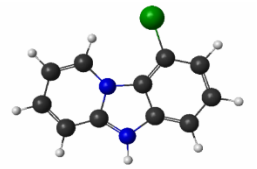

Number of atom	Charges on C	Boundary electron densities on C in HOMO	Charges on C (including solvation)	Boundary electron densities on C in HOMO (including solvation)
C^1	0.16595	0.05468	0.08589	0.06994
C^2	-0.13602	0.05678	-0.18660	0.06122
C^3	-0.04089	0.01222	-0.09491	0.01984
C^4	-0.10482	0.07300	-0.16754	0.08333
C^6	-0.09227	**0.20653**	-0.16762	**0.14518**
C^7	-0.07852	0.00110	-0.14530	0.00127
C^8	-0.07950	**0.21158**	-0.15275	**0.15638**

Analyses of the charges on the C atoms in the neutral (see Table 1) and nitrogen protonated molecule (see Table 2) showed the largest formal negative charge on the C^2 atom. According to the charge control, the probability of S_EAr reaction implementation by other reaction centres was lower one. This contradicted the experimental data obtained about the reaction proceeding in the 6th or 8th positions.

We further used the concept of electron density boundary distribution in the substrate molecule to explain the orientation of the electrophilic particle introduction into pyrido[1,2-*a*]benzimidazole **1**. The position in the substrate that has the highest electron density in the HOMO is most favoured for electrophilic attack in the S_EAr reaction [18]. The efficiency of the concept was demonstrated by evaluating the reactivity of condensed polyazaheterocycles in the S_EAr reaction [19].

The boundary electron densities in the HOMO on atoms (f_A) were estimated using the expression to compare the reactivity indices when a compound interacts with an electrophilic agent

$$f_A = 2\sum_{\mu \in A} C_{i\mu}^2, \qquad \textbf{(I)}$$

where $c_{i\mu}$ are the decomposition coefficients of the HOMO decomposition by AOs centred on atoms (A).

According to the data obtained, C^6 and C^8 atoms made the largest contribution to the electron density of the HOMO. The values of the coefficients on these atoms in neutral molecule **1** did not differ significantly. The differences between the contributions of C^6 and C^8 atoms increased considering the solvation environment of the molecule. The contribution difference between C^8 atom and C^6 atom to the electron density of the HOMO was further increased in the solvated **1'** cation molecule. Therefore, the position 8 of pyrido[1,2-*a*]benzimidazole should be the preferred centre for the attack of the electrophilic particle in the S_EAr reaction according to the concept of Fukui [15]. It agrees with the experimental data obtained (Table 3).

Table 3. Boundary electron densities on C atoms in the substrate HOMO and percentage content in the S_EAr reaction products in the reaction mass

The position of the electrophilic attack	C^6	C^8
Boundary electron densities on C in HOMO of solvated molecule 1'	0.14518	0.15638
Percentage content of bromination reaction products* **3a** and **4a**	32%	68%
Percentage content of chlorination reaction products* **3b** and **4b**	27%	73%

* - substrate and reagent were introduced into the reactor simultaneously.

Thus, the positions 6 and 8 of the heterocycle were the reaction centres in 9-chloropyrido[1,2-*a*]benzimidazole for electrophilic attack during the S_EAr reaction. The formation of 8,9-dihalogen derivative of pyrido[1,2-*a*]benzimidazole occurred to greater extent. The S_EAr reaction had orbital control according to quantum-chemical modelling data. The introduction orientation of the electrophilic particle was determined by the electron density boundary distribution in the substrate. The contribution of C^8 atom to the HOMO of the substrate was greater than the C^6 one. This correlated with the synthesis results.

Experimental part

We determined the melting points on a PolyTherm A device at a heating rate of 3 °C/min and did not adjust. NMR spectra were recorded on a Bruker Avance-II 600 spectrometer with operating frequencies of 600.13, 150.90 and 60.81 MHz for ^1H, ^{13}C and ^{15}N nuclei, respectively. A solvent was DMSO-d_6, internal standard was the residual solvent proton signal (δ 2.5) for the ^1H NMR spectrum and the ^{13}C DMSO-d_6 signal (δ 39.5) for the carbon spectra at 25 °C for **1** and 60 °C for **3a,b**. Heating for substances **3a,b** is related to the limited solubility of the compounds. Mass spectra were recorded on a FINNIGAN MAT instrument. INCOS 50, electron flux energy 70 eV.

Methodology for the synthesis of 9-chloropyrido[1,2-*a*]benzimidazole (1)

We added a solution of 2.50 g (0.00369 mol) of $SnCl_2$-$2H_2O$ in 15 ml of isopropanol at 35 °C to a solution of 1.00 g (0.00369 mol) of *N*-(2-nitro-6-chlorophenyl)pyridinium chloride in 15 ml of 4% HCl. We performed the reaction at 35 °C for 0.5 h. We then cooled the reaction mixture and treated with 25% NH_4OH to pH = 7-8 extracted with several portions of hot chloroform (Σ = 150 ml). We distilled off the solvent, obtaining the product as a beige coloured powder. Yield is 91%. T. melt. 101–103 °C. ^1H NMR (DMSO-d_6, δ, ppm, *J* /Hz): 9.27 (dt, *J* = 7.0, 1.2, 1H, H^1), 7.74 (dd, *J* = 8.2, 0.9, 1H, H^6), 7.67 (dt, *J* = 9.2, 1.2, 1H, H^4), 7.56 (ddd, *J* = 9.2, 6.6, 1.3, 1H, H^3), 7.42 (t, *J* = 7.9, 1H, H^7), 7.32 (dd, *J* = 7.7, 0.9, 1H, H^8), 6.98 (td, *J* = 6.8, 1.3, 1H, H^2). ^{13}C NMR (DMSO-d_6, δ, ppm.): 148.5 (C^{4a}), 145.8 (C^{5a}), 130.4 (C^3), 127.7 (C^1), 125.7 (C^7), 124.1 (C^{9a}), 121.6 (C^8), 118.0 (C^6), 117.4 (C^9), 117.1 (C^4), 110.8 (C^2). HRMS: *m/z* calculated $C_{11}H_7ClN_2$ 203.6396 $[M+H]^+$, found 203.6391.

Methodology for the synthesis of 8-Hal-9-chloropyrido[1,2-*a*]benzimidazoles (3a,b)

We added a solution of 2.00 g (0.01 mol) of 9-chloropyrido[1,2-*a*]benzimidazole in 25 ml H_2SO_4 to a solution of 2.5 g (0.014 mol) of N-bromosuccinimide (**2a**) for the synthesis of **3a** or 4.0 g (0.03 mol) of N-chlorosuccinimide (**2b**) for the synthesis of **3b** in 50 ml of H_2SO_4 at 35 °C for 10 h, followed by stirring for another 10 h at 40-45 °C. Then we poured the mixture into ice and treated it with 25% NH_4OH to pH = 7-8. The beige precipitate was filtered off, washed with cold water and dried.

8-Bromo-9-chloropyrido[1,2-*a*]benzimidazole (**3a**) Yield is 89%. T. melt. 121–124 °C. ^{1}H NMR spectrum (DMSO-d_6, δ, ppm, *J*/Hz): 9.35 (d, 1H, H^{1}, *J* = 7.3), 7.76 (d, 1H, H^{4}, *J* = 8.5), 7.69 (m, 2H, H^{6,7}), 7.62 (t, 1H, H^{3}, *J* = 7.9), 7.05 (t, 1H, H^{2}, *J* = 6.9). ^{13}C NMR (DMSO-d_6, δ, ppm): 148.8 (C^{4a}), 143.9 (C^{5a}), 130.6 (C^{3}), 127.4 (C^{1}), 126.3 (C^{7}), 124.9 (C^{9a}), 123.6 (C^{8}), 119.4 (C^{6}), 117.2 (C^{4}), 115.8 (C^{9}), 111.1 (C^{2}). HRMS: *m/z* calculated $C_{11}H_6BrClN_2$ 282.5357 $[M+H]^+$, found 282.5352.

8,9-dichloropyrido[1,2-*a*]benzimidazole (**3b**). Yield is 87%. T. melt. 131–135 °C. ^{1}H NMR (DMSO-d_6, δ, ppm, *J*/Hz): 9.27 (dt, *J* = 7.1, 1.2, 1H, H^{1}), 7.69 (d, *J* = 8.7 Hz, 1H, H^{6}), 7.65 (dt, *J* = 9.2, 1.2, 1H, H^{4}), 7.59 – 7.55 (m, 2H, H^{3}, H^{7}), 7.00 (td, *J* = 6.9, 1.3, 1H, H^{2}). ^{13}C NMR (DMSO-d_6, δ, ppm): 148.8 (C^{4a}), 143.9 (C^{5a}), 130.4 (C^{3}), 127.2 (C^{1}), 126.2 (C^{7}), 124.9 (C^{9a}), 123.5 (C^{8}), 118.4 (C^{6}), 117.0 (C^{4}), 115.7 (C^{9}), 111.0 (C^{2}). HRMS: *m/z* calculated $C_{11}H_6Cl_2N_2$ 238.0847 $[M+H]^+$, found 238.0841.

Calculation part

We performed quantum-chemical electronic structure calculations using the PC GAMESS/Firefly software package and the ORCA 5.0.4 programme. We used PC GAMESS/Firefly to optimise the geometry of compound **1** and its imide nitrogen protonated heterocycle derivative **1'** in the gas phase. The ORCA software was used to optimise the geometry of **1** and **1'** taking into account the solvate shell. We considered the impact of the medium using the electron density solvation model (SMD). The electronic parameters of the molecule were calculated in the framework of density functional theory with a hybrid exchange-correlation functional (DFT method B3LYP/6-31G**) for open electron shells. The boundary electron densities in the HOMO on carbon atoms (f_A) were calculated according to formula (**I**). We used the programs wxMacMolPlt [20] and ChemCraft [21] to process the data and visualise the calculation results.

References

1. **Mayoka, G., Keiser, J., Häberli, C. & Chibale K.** (2019) Structure–Activity Relationship and *in Vitro* Absorption, Distribution, Metabolism, Excretion, and Toxicity (ADMET) Studies of N-aryl 3-Trifluoromethyl Pyrido[1,2-*a*]benzimidazoles That Are Efficacious in a Mouse Model of Schistosomiasis, *ACS Infect. Dis.,* 5, pp. 418–429. DOI: 10.1021/acsinfecdis.8b00313.
2. **Liu, A., Ji, R., Shen, S., Cao, X. & Ge,Y.** (2017) A ratiometric fluorescent probe for sensing sulfite based on a pyrido [1, 2-a] benzimidazole fluorophore, *New Journal of Chemistry,* 41(18), pp. 10096-10100. DOI: 10.1039/C7NJ02086D.
3. **Gadde, S., Kleynhans, A., Holien, J.K., Bhadbhade, M., Nguyen, P.L.D., Mittra, R., Yu, T.T., Carter, D.R., Parker, M.W., Marshall, G.M., Cheung, B.B. & Kumar, N.** (2023) Pyrimido[1,2-*a*]benzimidazoles as inhibitors of oncoproteins ubiquitin specific protease 5 and MYCN in the childhood cancer neuroblastoma, *Bioorg Chem.,* 136, 106462. DOI: 10.1016/j.bioorg.2023.106462.
4. **Kotovskaya, S.K., Baskakova, Z.M., Charushin, V.N., Chupakhin, O.N., Belanov, E.F., Bormotov, N.I., Balakhnin, S.M. & Serova, O.A.** (2005) Synthesis and antiviral activity of fluorinated pyrido[1,2-*a*]benzimidazoles, *Him.-farm. Zhurnal,* 39(11), pp. 12–16. DOI: 10.30906/0023-1134-2005-39-11-12-16 (in Russian).

5. **Arutyunyan, A.A., Avakimyan, J.A. & Stepanyan, G.M.** (2016) Antibacterial properties of some polycyclic heterocycles based on pyrimidine and benzimidazole, *Biologicheskij zhurnal Armenii,* 68(2), pp. 88-91 [online]. Available at: https://arar.sci.am/dlibra/publication/260297 (accessed 02.02.2024) (in Russian).
6. **Koo, H.L. & Dupont, H.L.** (2010) Rifaximin: A Unique Gastrointestinal-Selective Antibiotic for Enteric Diseases, *Curr. Opin. Gastroenterol.,* 26, pp. 17–25. DOI: 10.1097/MOG.0b013e328333dc8d.
7. **Begunov, R.S., Egorov, D.O., Chetvertakova, A.V., Savina, L.I. & Zubishina, A.A.** (2023) Antibacterial Activity of the Halogen- and Nitro Derivatives of Benzimidazole Against Bacillus Subtilis, *Antibiotiki i khimioterapiya,* 68(3-4), pp. 19-24. DOI: 10.37489/0235-2990-2023-68-3-4-19-24 (in Russian).
8. **Andrzejewska, M., Yépez-Mulia, L., Cedillo-Rivera, R., Tapia, A., Vilpo, L., Vilpo, J. & Kazimierczuk, Z.** (2002) Synthesis, antiprotozoal and anticancer activity of substituted 2-trifluoromethyl- and 2-pentafluoroethylbenzimidazoles, *European Journal of Medicinal Chemistry,* 37, pp. 973–978. DOI: 10.1016/S0223-5234(02)01421-6.
9. **Tkachenko, P.V., Tkachenko, E.V., Zhuravel, I.A., Kazmirchuk, V.V. & Derbisbekova, U.B.** (2017) Synthesis and antimicrobial activity 4-arylsulphonyl-derivatives 5-aminopyrazoles, *Vestnik KazNMU,* (2), pp. 307–311 [online]. Available at: https://cyberleninka.ru/article/n/sintez-i-protivimikrobnaya-aktivnost-4-arilsulfonilproizvodnyh-5-aminopirazolov (accessed 12.02.2024) (in Russian).
10. **Begunov, R.S., Sokolov, A.A., Belova, V.O., Fakhrutdinov, A.N., Shashkov, A.S. & Fedyanin, I.V.** (2015) Reaction of substituted pyrido[1,2-*a*]benzimidazoles with electrophilic agents, *Tetrahedron Letters,* 56(42), pp. 5701–5704. DOI: 10.1016/j.tetlet.2015.08.014.
11. **Begunov, R.S., Ryzvanovich, G.A. & Firgang, S.I.** (2004) Simple method for the synthesis of substituted benzo[4,5]imidazo[1,2-*a*]pyridines, *Zhurnal organicheskoj khimii*, 40(11), pp. 1740-1742. DOI: 10.1007/s11178-005-0082-5 (in Russian).
12. **Bogdanova, D.M., Savina, L.I. & Begunov, R.S.** (2022) Synthesis and functionalization of pyrido[1,2-*a*]benzimidazole amino derivatives, *From Chemistry Towards Technology Step-By-Step,* 3(4), pp. 30-38 [online]. Available at: http://chemintech.ru/index.php/tor/2022-3-4 (in Russian) (accessed 10.12.2023).
13. **Becke, A. D.** (1993) Density-functional thermochemistry. III. The role of exact exchange, *J. Chem. Phys.,* 98(7), pp. 5648-5652. DOI: 10.1063/1.464913.
14. **Miehlich, B.A., Savin, H.S., Stoll, H. & Preuss, H.** (1989) Results Obtained with the Correlation Energy Density Functionals of Becke and Lee, Yang and Parr, *Chemical Physics Letters,* 157(3), pp. 200-206. DOI: 10.1016/0009-2614(89)87234-3.
15. **Mueller, M.** (2001) Fundamentals of Quantum Chemistry. Molecular Spectroscopy and Modern Electronic Structure Computation, *International Journal of Molecular Sciences,* 2(6), pp. 291-292. DOI: 10.3390/i2060291.
16. **Granovsky, A.A.** (2024) Firefly version 8.8 [online]. Available at: http://classic.chem.msu.su/gran/firefly/index.html (accessed 20.02.2024).
17. **Neese, F.** (2012) The ORCA program system, *Wiley Interdisciplinary Reviews: Computational Molecular Science,* 2(1), pp. 73–78. DOI: 10.1002/wcms.81.
18. **Fukui, K., Yonezawa, T. & Nagata, C.** (1957) MO-Theoretical Approach to the Mechanism of Charge Transfer in the Process of Aromatic Substitutions, *Bulletin of the Chemical Society of Japan,* 27, pp. 1247–1256. DOI: 10.1063/1.1743986.
19. **Breza, M. & Milata, V.** (2005) Quantum-chemical studies of the nitration of benzazoles, *ARKIVOC,* 9, pp. 80-89. DOI: 10.3998/ark.5550190.0006.909.
20. **Bode, B.M. & Gordon, M.S.** (1998) MacMolPlt: a graphical user interface for GAMESS, *J. Mol. Graphics and Modeling,* 16(3), pp. 133-138. DOI: 10.1016/s1093-3263(99)00002-9).
21. **Zhurko, G.A.** (2024) Chemcraft. Version 1.6 [online]. Available at: http://www.chemcraftprog.com (accessed at 12.02.2024).

Received 14.05.2024
Approved 31.05.2024
Accepted 31.05.2024